Catalysis Today 144 (2009) 42–47

Contents lists available at ScienceDirect

Catalysis Today

journal homepage: www.elsevier.com/locate/cattod

Photo-assisted degradation of 2-propanol in gas–solid regime by using TiO_2 impregnated with heteropolyacid $H_3PW_{12}O_{40}$

G. Marcì *, E. García-López, L. Palmisano

"Schiavello-Grillone" Photocatalysis Group, Dipartimento di Ingegneria Chimica dei Processi e dei Materiali, Università di Palermo, Viale delle Scienze, 90128 Palermo, Italy

ARTICLE INFO

Article history:
Available online 4 January 2009

Keywords:
Polyoxometalate
2-Propanol
Heterogeneous photocatalysis
TiO_2

ABSTRACT

Commercial and home prepared TiO_2 samples impregnated with tungstophosphoric acid ($H_3PW_{12}O_{40}$) were used for the photo-assisted degradation of 2-propanol in gas–solid regime. The characterization results evidenced a good coverage of the polyoxometalate (POM) onto the surface of TiO_2 along with a marginal effect of the presence of the POM on the specific surface area, morphology and cristallinity of the samples. Propene was the main intermediate product revealed in 2-propanol photocatalytic degradation by using as photocatalysts the samples containing the POM, whereas propanone was mainly obtained when the photocatalysts was bare TiO_2, both commercial or home prepared. Acetaldehyde was also found as an intermediate product along with traces of isopropyl ether, mesityl oxide and isobutyl-methyl-ketone that were also detected as gaseous products in all the runs. Carbon dioxide and water were the ultimate oxidation products.

1. Introduction

The heteropolyacids, which belongs to the huge family of the polyoxometalates (POMs), are very strong Brönsted acids and efficient oxidants that perform fast and reversible redox multi-eletronic transformations in mild conditions; consequently they can act as bifunctional catalysts used in solution as acid and oxidation catalysts. They have well defined structures and properties, their size are typically few nanometers and, due to the fact that they are very soluble in polar solvents, POMs have been used extensively in homogeneous catalysis being able to activate molecular oxygen or hydrogen peroxide as reagents in oxidation reactions [1]. Misono et al. report that when POMs are used as catalysts the nature of the reactants determines whether the reaction occurs on the surface of the catalysts or in the bulk. When the reactant is a polar molecule POMs absorb it into their bulk, leading to a pseudo-liquid phase type of catalysis; on the contrary when the substrate is an apolar molecule the reaction occurs only on the surface or between surface layers of the crystal [2]. POMs share photochemical characteristics with semiconductor photocatalysts [3]; indeed, both classes of materials are constituted by d^0 transition metal and oxide ions and exhibit similar electronic characteristics (HOMO–LUMO transition for the POMs and band-gap transition for semiconductors). Hence, POMs not only are bifunctional acid–base and redox catalysts but also they can be activated by light and photo-assisted oxidation reactions, carried out in liquid phase, using the heteropolyacid $H_3PW_{12}O_{40}$ homogeneous catalyst can occur [4]. Some attempts have been made to heterogenise these materials by using as supports silica MCM41 [5], resins [6] or the polysiloxane polymer [7].

Photocatalysis is a field of great interest that in the last decades has been studied mainly for the abatement of pollutants present in gaseous or liquid stream. Some authors report also the use of photocatalysts consisting of heteropolyacid supported on TiO_2 [8] or ZrO_2 [9] where a synergistic effect is observed between the two materials, ascribing this improvement to the delaying of the electron–hole recombination [10]. The transfer of electrons from POM to oxygen species present in the reaction medium should enhance the reaction kinetics, as evidenced by spectroscopic studies [11]. Due to its (photo)stability and low cost, the most used photocatalyst is titanium dioxide [12]. Its photoactivity strongly depends on several variables as preparation method, particle size, reactive surface area, ratio between anatase and rutile phases. A way to improve the activity of a photocatalyst is to increase its specific surface area and to decrease the size of the particles, even if the diminuition of the dimension could increase photon scattering which is a negative effect, reasons for which much attention has been devoted to nanostructured TiO_2 materials [13]. Various nanostructured TiO_2 catalysts prepared by hydrolysis of titanium tetrachloride show a good photocatalytic activity [14] and in their preparation neither filtration nor calcination is needed to obtain a highly efficient anatase phase.

* Corresponding author.
E-mail address: marci@dicpm.unipa.it (G. Marcì).

0920-5861/$ – see front matter © 2008 Published by Elsevier B.V.
doi:10.1016/j.cattod.2008.11.010

The photocatalytic degradation of 2-propanol in the presence of both oxygen and UV light at ambient temperature has been used as a probe reaction in the presence of TiO_2 as the photocatalyst. In literature, propanone is reported to be the only intermediate product in the photocatalytic oxidation of 2-propanol both in gas–solid regime [15–17] and in liquid–solid one [18–20], followed by subsequent photo-oxidation to produce ultimately CO_2. The use of modified TiO_2, for instance by incorporating sulfuric acid during the photocatalysts preparation, leads to a high selectivity versus the formation of isoproylether [21]. Moreover, it is accepted that a good reaction to probe the acid character of a catalyst is 2-propanol dehydration in the gas–solid regime to give propene at ambient pressure and at moderate temperature (in the range 140–220 °C). The reaction occurs through a two-step E1 mechanism due to the high stability of the tertiary carbocation formed during the reaction. However the dehydrogenation pathway can also occur giving rise to propanone. The selectivity to propene or to propanone strongly depends on the experimental conditions, mainly temperature and gaseous ambient phase (He, N_2, H_2, O_2) and the acidity–basicity of the solid catalyst, thus the degradation of this substrate has been proposed as a test reaction to determine the acid–base properties of an oxide catalyst [22].

The objective of this work is the preparation of binary photocatalysts consisting of POM supported onto TiO_2. Two types of TiO_2, commercial and home prepared powders were impregnated with the Keggin type heteropolyacid $H_3PW_{12}O_{40}$. This investigation has been focused on the role of the POM on the photocatalysts physico-chemical characteristics and on their photocatalytic activity and selectivity versus the intermediate species obtained during the photo-degradation of 2-propanol.

2. Experimental

2.1. Preparation and characterization of the binary solids

Titanium tetrachloride (Fluka 98%) was used as the starting material without any further purification to obtain the home prepared TiO_2. $TiCl_4$ was slowly added to distilled water (volume ratio 1:50) at room temperature [14]. The hydrolysis reaction was highly exothermic. After ca. 1 h of continuous stirring, the resulting solution was refluxed for 24 h. After the refluxing treatment the obtained opalescent dispersion was evacuated in a rotavapor to obtain a powder (called TiO_2 home prepared or just hp). No calcination step was accomplished. Both commercial (Degussa P25) and home prepared TiO_2 were successively impregnated by incipient wetness with an aqueous solution of a commercial polyoxometallate, tungstophosphoric acid $H_3PW_{12}O_{40}$ (Aldrich reagent grade 99.7%), named POM in the following. The molar ratio Ti:POM was held constant at 1:0.01. The final mixture containing both the TiO_2 and POM was evaporated until dryness. An annealing treatment at 120 °C under vacuum (ca. 0.1 Torr) was eventually performed.

The powders obtained were labelled as POM/ followed by the acronym P25 (TiO_2 Degussa P25) or hp (TiO_2 home prepared), indicating the type of TiO_2 present in the binary solid catalyst.

The solid samples were characterised by X-ray diffractometry (XRD) recorded at room temperature by a Philips powder diffractometer using the Cu Kα radiation and a 2θ scan rate of 2°/min. Determinations of BET specific surface area (SSA) were carried out by using a Micromeritics Flowsorb 2300 Instrument. Scanning electron microscopy (SEM) observations were performed using a Philips XL30 ESEM microscope, operating at 25 kV on specimens upon which a thin layer of gold had been evaporated. An electron microprobe used in an energy dispersive mode (EDX) was employed to obtain information on the atomic content of W on the samples. Diffuse reflectance spectra (DRS) were recorded in the range 250–600 nm by using a Shimadzu UV-2401 PC instrument with $BaSO_4$ as the reference sample. Infrared spectra of the samples in KBr (Aldrich) pellets were obtained with a FTIR-8400 Shimadzu and the spectra were taken with 4 cm^{-1} resolution and 256 scans.

2.2. Photoreactivity experiments

The photoreactor operating in gas–solid regime was a continuous Pyrex fixed bed photoreactor of cylindrical shape (diameter 58 mm, height 100 mm) [23]. A porous glass septum at the bottom of the cylinder allowed to sustain the fixed bed of the solid and to distribute the inlet gaseous mixture. The corresponding fixed bed height was ca. 1 mm. The reactivity runs were carried out with 1.5 g of photocatalyst. The gas feeding the photoreactor consisted of oxygen, 2-propanol and water. 2-Propanol and water were introduced in the oxygen stream by means of a home made infusion pump. The amounts of 2-propanol and water injected into the oxygen stream were such that they instantaneously vaporized at the temperature of 298 K. The initial concentration of 2-propanol in gas phase was 8×10^{-5} M and the water concentration was 3.4×10^{-4} M (relative humidity percentage ca. 27%). Water was absent during the course of some selected runs in order to study its influence in the reaction. Preliminary tests were performed with the aim of determining the suitable flow rate conditions to avoid mass transport limitations on the photoreaction and consequently the flow rate at which the runs were eventually carried out was 0.5 $cm^3\ s^{-1}$. The irradiation started after ca. 1 h, i.e. only when steady state conditions were achieved under dark conditions.

The reactor was vertically positioned and illuminated from the top inside a SOLARBOX apparatus (CO.FO.ME.GRA.) equipped with solar simulating Xe lamp of 1500 W. A water filter was located between the lamp and the photoreactor to cut-off the infrared radiation and to maintain the temperature inside the reactor at ca. 300 K. The irradiance reaching the photoreactor was measured by using a *UVX Digital* radiometer and it was equal to 1.0 mW cm^{-2} in the radiation wavelengths range between 355 and 375 nm. The runs lasted ca. 6 h and samples of the reacting fluid were analyzed by withdrawing at fixed intervals of time 200 μl of gas from the outlet of the photoreactor by means of a gas-tight syringe. Substrate and intermediate products concentrations were measured by a GC-17A Shimadzu gas chromatograph equipped with a HP-1 column and a FID, whereas carbon dioxide was analyzed by a Carboxen column in an HP6890 gas chromatograph equipped with a TCD.

3. Results and discussion

3.1. Physico-chemical characterisation

The diffractograms of the home prepared TiO_2 samples, not shown for the sake of brevity, indicate the presence of incomplete crystallised anatase and rutile phases. The size of the crystallites, estimated by means of the Scherrer equation, were in the range 10–20 nm for anatase and 5–8 nm for rutile. No significant differences were observed by studying the home prepared TiO_2 samples impregnated with POM even after the vacuum-annealing treatment. Also the samples obtained by impregnation of TiO_2 Degussa P25 showed X-ray diffractograms very similar to that obtained for the bare commercial TiO_2. No peaks corresponding to POM were observed whatever impregnation medium was used, indicating, in any case, a very good dispersion of POM onto the titanium dioxide surface.

The specific surface areas of the samples based on TiO_2 home prepared were 51 and 49 $m^2\ g^{-1}$ for TiO_2 hp and POM/hp, respectively. The specific surface area of TiO_2 Degussa P25 was

45 $m^2 g^{-1}$ whereas the value obtained for POM/P25 was 38 $m^2 g^{-1}$. It is clear that the surface area of the POM loaded samples resulted slightly lower on respect to the bare TiO_2. This slight decrease can be attributed to the coverage of the TiO_2 surface with the tungstophosphoric acid molecules suggesting that the POM units are dispersed onto the TiO_2 surface.

SEM observations revealed that all the samples consisted of aggregates of particles. From the observation of the micrographs, not reported for the sake of brevity, it is evident that the loading of TiO_2 with POM modified neither the morphology nor the particles size, that were in the range of 70–150 nm for the home prepared TiO_2, both bare and loaded with POM. Micrographs obtained for bare and loaded TiO_2 Degussa P25 showed aggregates of particles whose size were in the range 70–150 and 120–150 nm, respectively.

EDX measurements confirmed a homogeneous distribution of the POM onto the surface of the TiO_2 support. The atomic percentage amount of tungsten measured by EDX was 13.0% and 13.5% for POM/hp and POM/P25, respectively. This figure was slightly bigger than that of the nominal one (11% atoms of W on respect to the total amount of Ti + W), indicating that POM was deposited onto the TiO_2 surface. EDX analysis showed also that the amount of chloride ions present in the bare TiO_2 home prepared sample was less than 0.2%.

The diffuse reflectance spectra of the samples, showed in Fig. 1, are quite similar each other with a broad absorption band, ascribed to the charge transfer process O^{2-} to Ti^{4+} responsible of the band-gap. TiO_2 is an indirect semiconductor [24] and the band gap energies of the samples have been estimated from the tangent lines in the plots, not shown for the sake of clarity, of the modified Kubelka–Munk function, $[F(R'_\infty)h\nu]^{1/2}$, versus the energy of exciting light [25]. The values ranged between 3.0 and 3.2 eV. It can be noticed a slight decrease of reflectance (i.e. increase of absorbance) in the visible region by adding the POM to commercial and home prepared TiO_2 samples. The bathochromic shift of this electron transfer band is observed for all of the samples containing the POM species on the TiO_2 surface.

The solid samples were analyzed by FTIR in order to confirm the structural integrity of the Keggin unit on the TiO_2 surface. The structure of the $PW_{12}O_{40}{}^{3-}$ anion consists in PO_4 tetrahedron surrounded by four W_3O_{23} groups formed by edge sharing octahedra. These groups are connected to each other by corner sharing oxygen atoms [26]. This arrangement gives rise to four types of stretching bands between 1100 and 700 cm^{-1}, the fingerprint region for this kind of compounds. The presence of the TiO_2 cut-off at wavelengths lower than 900 cm^{-1} does not allow to clearly observe some of these bands. Fig. 2 shows the FTIR spectra of the POM loaded TiO_2 samples along with the bare POM.

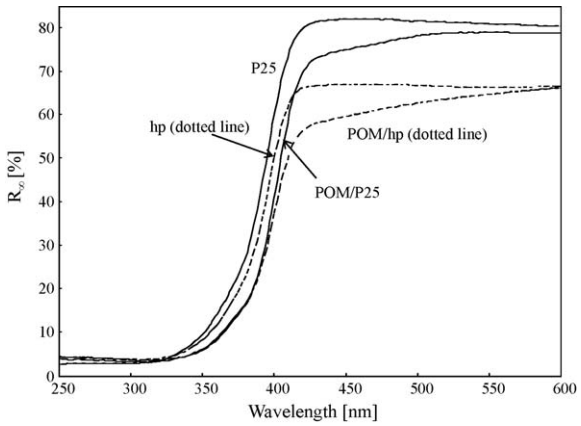

Fig. 1. Diffuse reflectance spectra of bare TiO_2 and POM loaded samples.

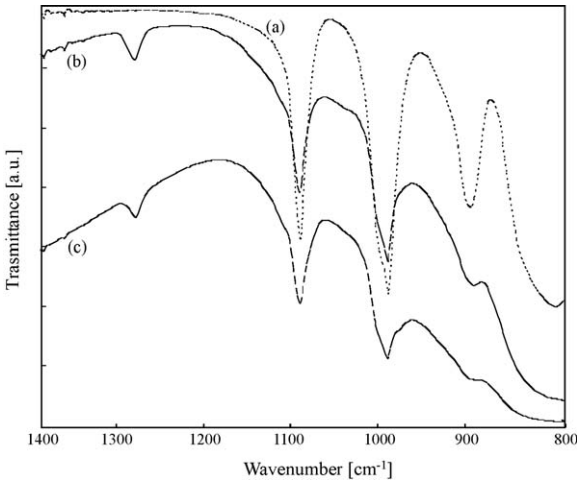

Fig. 2. FT-IR spectra of KBr pellets of: (a) commercial $H_3PW_{12}O_{40}$; (b) POM/P25; (c) POM/hp.

It is clear that the four main stretching vibrations of the skeletal bonds in PW_{12} are located at ca. the same wavenumbers found when the POM is loaded on the surface of both commercial and home prepared TiO_2, indicating that the Keggin geometry of PW_{12} was still preserved in the binary material. The typical band for P–O absorption (1080 cm^{-1}) is displayed, along with the stretching W=O (990 cm^{-1}). The two peaks that appear at ca. 890 and 810 cm^{-1} [27] can be attributed to two types of W–O–W and they are partially covered by cut-off of the titanium dioxide.

The bands attributed to the Keggin's unit skeletal vibrations did not become sharper in the samples where the POM was supported on the TiO_2, as expected when absence of anion-anion interactions occurs, on respect to those attributed to the bare POM [27,28]. This insight could be attributed to the interactions between the Keggin units and the surface of the TiO_2, considering the relative low amount of POM and its homogeneous dispersion onto the support surface. In fact, the H-bonding interactions between the Keggin units and the TiO_2 cannot be excluded, particularly considering the broadening of the bands that could indicate that the vibrations are disturbed by dipole–dipole interactions [28].

3.2. Photoreactivity experiments

Blank reactivity tests were performed under the same experimental conditions used for the photo-reactivity experiments but in the absence of catalyst, oxygen or light. No reactivity was observed in all these cases so that it was concluded that the contemporary presence of O_2, catalyst, and irradiation is needed for the occurrence of the 2-propanol degradation process. The solid samples showed strong absorption of the substrate and ca. 1 h was necessary to achieve steady state conditions.

Fig. 3 reports the values of the outlet 2-propanol concentration vs. irradiation time for some selected runs carried out by using TiO_2 Degussa P25, POM/P25, TiO_2 hp and POM/hp as the photocatalysts. The initial increase of 2-propanol observed for the runs carried out in the presence of POM/P25, TiO_2 hp and POM/hp (Fig. 3(b)–(d)) can be attributed to the photo/thermal desorption of the substrate adsorbed during the stabilization period under dark, just after switching on the lamp. A successive decrease in the concentration of 2-propanol was observed for all the runs. 2-Propanol completely disappeared in the course of the reaction only in the presence of TiO_2 Degussa P25. During the course of all the runs the disappearance of the substrate was observed along with a simultaneous formation of propanone, propene and acetaldehyde, although the last one was obtained in very small amounts. In

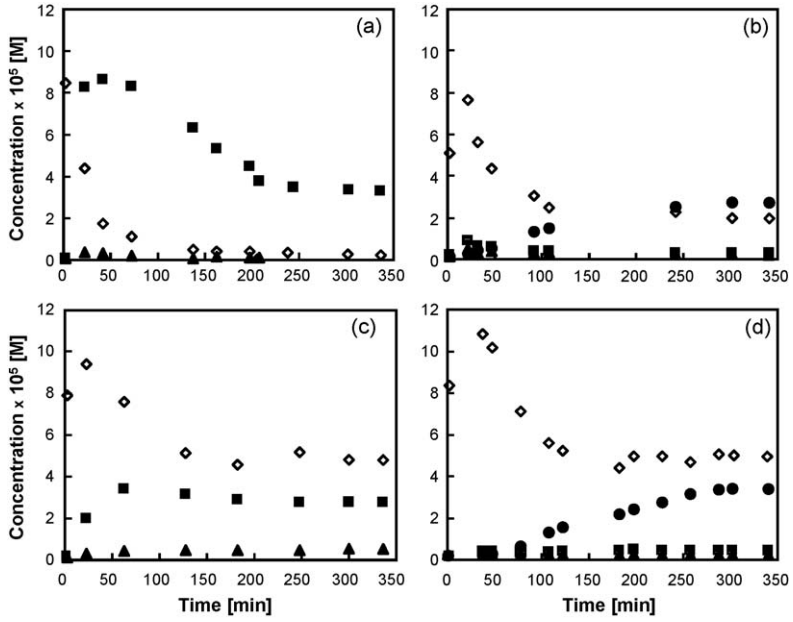

Fig. 3. Evolution of 2-propanol (◇), propanone (■), propene (●) and acetaldehyde (▲) concentrations vs. irradiation time for reaction in the gas–solid system in the presence of: (a) TiO_2 Degussa P25; (b) POM/P25; (c) TiO_2 hp; (d) POM/hp.

particular, propanone formed in the presence of both the bare TiO_2 Degussa P25 and TiO_2 hp samples, while propene was found as the main intermediate in all the runs carried out in the presence of POM loaded photocatalysts. Traces of isopropyl ether, mesityl oxide and isobutyl-methyl-ketone were also detected as gaseous products. It is worth noting that the concentration of all the intermediate products reached a steady state value after a time depending on the photocatalyst used. Moreover, under the current experimental conditions, carbon dioxide was contemporaneously produced.

A perusal of Fig. 3 reveals that the presence of the POM onto the TiO_2 surface strongly influences the photo-catalytic behaviour of the TiO_2 bare samples; indeed, due to the increased surface acidity, the selectivity of the POM-TiO_2 binary catalyst towards the propene formation increased whereas it drastically decreased towards propanone.

Table 1 reports the 2-propanol disappearance rate ($r_{2\text{-propanol}}$) and its conversion along with the yield in propanone, propene, acetaldehyde, isopropylether and CO_2 for runs carried out by using TiO_2 Degussa P25, POM/P25, TiO_2 hp and POM/hp. The 2-propanol disappearance rate ($r_{2\text{-propanol}}$) was calculated by applying the following mass balance equation on the whole photoreactor:

$$r_{2\text{-propanol}} = W \cdot (C^0_{2\text{-prop}} - C_{2\text{-prop}}) \quad (1)$$

in which W is the volumetric gas flow rate and $C^0_{2\text{-prop}}$ and $C_{2\text{-prop}}$, the inlet and outlet 2-propanol molar concentrations, respectively.

The perusal of Table 1 reveals that the reaction rate for 2-propanol degradation is maximum by using TiO_2 Degussa P25. It resulted 2.4 times higher than that obtained in the presence of TiO_2 hp. 2-Propanol degradation rate was the same by using POM/P25 and POM/hp even if it was slower than that obtained by using TiO_2 Degussa P25 and faster than that obtained by using TiO_2 hp. This result evidences that the presence of POM gave rise to an enhancement of the activity of TiO_2 hp and to a decrease of that of TiO_2 Degussa P25. As far as selectivity is concerned, the photo-oxidation runs indicated that 2-propanol degradation occurred via the formation of various intermediates whose amount depended on the type of photocatalyst used. Those found in significant amounts were propanone and acetaldehyde by using TiO_2 Degussa P25. Propene, propanone and in a lesser extent acetaldehyde were revealed when TiO_2 hp, POM/P25 and POM/hp were used.

The amount of propene increased dramatically by using both the loaded POM photocatalysts. Moreover, the percentage of mineralization of 2-propanol to CO_2 increased by using the POM/hp sample. These results can be explained by taking into account the different nature of the surface sites on the photocatalysts in terms of acidity/basicity of the powders. In fact, it is generally proposed that propene formation involves either surface Brönsted or Lewis acid sites, leading to hydrogen bonded or coordinated 2-propanol species respectively. The E1 mechanism requires only very strong acid sites, responsible for the formation of olefins, whereas the E2 mechanism, involving both the acid and the basic sites of the solid, leads to the formation of the ether [22]. Propene can be also formed by an intermolecular dehydration and the

Table 1
Reactivity results for 2-propanol disappearance. The values reported correspond to the percentage of conversion, X (%), after 6 h of irradiation along with the selectivity towards the intermediates and the final product (CO_2).

	r (mol s^{-1})[a]	X (%)[a]	Selectivity (%)[a]				
			Propanone	Propene	Acetaldehyde	Isopropylther	CO_2
POM/P25	2.5×10^{-8}	75	14	78	3	2	2
POM/hp	2.5×10^{-8}	60	6	66	1	3	23
TiO_2 Degussa P25	4.1×10^{-8}	99	47	0	1	0	50
TiO_2 hp	1.7×10^{-8}	43	79	0	11	0	10

[a] The reported values are the average of three measurements.

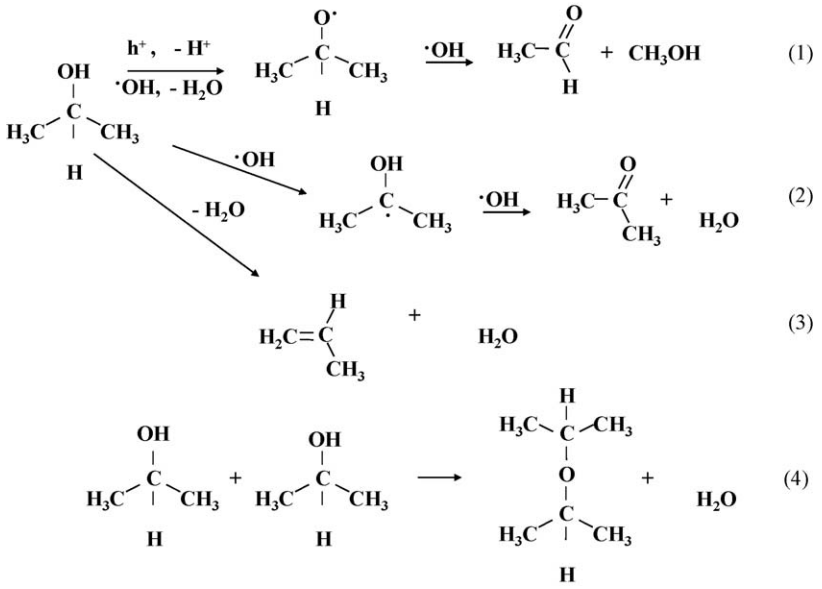

Scheme 1. Hypothesized reaction pathway for 2-propanol photocatalytic oxidation in the presence of bare TiO_2 and/or POM/TiO_2.

reaction needs acidic OH groups. The intermolecular dehydration is easier than the intramolecular one that gives rise to the formation of isopropylether. These physico-chemical aspects related to the photocatalysts reactivity will be focused in a future work.

There is an agreement in the literature to consider that the main gaseous products in the 2-propanol photocatalytic oxidation by using TiO_2 are propanone, CO_2 and H_2O. Our results are in agreement with previous work in which also acetaldehyde was found as intermediate in the photocatalytic degradation of 2-propanol [15]. Moreover, in the present work, propene was found due to the strong acidic character of the binary POM-TiO_2 loaded samples. The present results suggest the occurrence of different photodegradation pathways, as reported in Scheme 1.

The generated $^{\bullet}OH$ radicals, produced as already well known in photocatalytic processes [12], can react with 2-propanol. It could be considered the formation of two different radicals: $(CH_3)_2CHO^{\bullet}$ and $(CH_3)_2C^{\bullet}OH$ (reactions (1) and (2)). These radical species could evolve, through several reaction steps, to acetaldehyde and propanone, respectively. The presence of methanol as a reaction product, suggested in reaction (1), was not observed in the reacting medium, probably because it can be quickly decomposed to CO_2. As far as the propene molecule formation is concerned, as reported in reaction (3), it could derive from the dehydration of the adsorbed 2-propanol in an appropriate acidic surface site. Probably the UV light is able to supply the energy that in the catalytic reaction is provided by heating the system. The formation of isopropylether can be explained by considering reaction (4) that involves an intramolecular dehydration of two 2-propanol molecules.

In order to study the influence of the presence of water vapour (3.4×10^{-4} M) on the photoreactivity, some experiments were carried out in its absence, concluding that the presence of water, in the experimental conditions used, was irrelevant, as far as reaction rate, conversion and yield in the intermediates are concerned. This finding can be explained by considering the formation of water as a reaction product [15–20]. As reported in literature, the presence of water is necessary in order to displace propanone from the surface [29] and we hence conclude that the amount of water produced during the reaction is enough to allow the restoration of the active sites. The behaviour of 2-propanol contrasts with that observed with some probe aromatic molecules such as toluene [23] for which deactivation of the photocatalyst occurred also in the presence of water in gas–solid system by using TiO_2 Degussa P25, due to a strong interaction of produced benzoate species onto the surface sites [30].

4. Conclusions

The photocatalytic degradation of 2-propanol occurred successfully in gas–solid regime by using commercial and home prepared TiO_2 impregnated with $H_3PW_{12}O_{40}$. Propanone and propene were the main intermediate products while acetaldehyde and isopropylether showed to be minor intermediates. Carbon dioxide and water were the main oxidation products. Home prepared TiO_2, obtained by hydrolysis of $TiCl_4$, consisted of badly crystallized anatase and rutile particles and the impregnation with $H_3PW_{12}O_{40}$ produced samples where POM resulted well dispersed onto the surface of TiO_2 and where the Keggin geometry of the PW_{12} was still preserved.

Photoreactivity experiments have shown that 2-propanol degradation rate by using the commercial TiO_2 Degussa P25 was 2.4 faster than that using the home prepared TiO_2 samples. The activity of the home prepared TiO_2 was enhanced by the impregnation with the POM, whereas it was depleted for TiO_2 Degussa P25. The distribution of the intermediate products changed dramatically. By using both the bare TiO_2 samples, the main intermediate product was propanone, whereas when the binary material POM/TiO_2 was used as the photocatalyst, propene was found as the main intermediate product. The different selectivity can be ascribed to differences in the physico-chemical characteristics of the solid surface.

Acknowledgement

The authors wish to thank MIUR (Rome) for financial support.

References

[1] I.V. Kozhevnikov, Chem. Rev. 98 (1998) 171.
[2] N. Mizuno, M. Misono, Chem. Rev. 98 (1998) 199.
[3] A. Hiskia, A. Mylonas, E. Papaconstantinou, Chem. Soc. Rev. 30 (2001) 62.
[4] P. Kormali, A. Troupis, T. Triantis, A. Hiskia, E. Papaconstantinou, Catal. Today 124 (2007) 149.

[5] M.J. Verhoet, P. Kooyman, J.A. Peters, H. VanBekkum, Micropor. Mesopor. Mater. 27 (1999) 365.
[6] A.L. Villa, P.B. Sels, D.E. De Vos, P.A. Jacobs, J. Org. Chem. 64 (1999) 7267.
[7] E. Fontananova, L. Donato, E. Drioli, L.C. López, P. Favia, R. D'Agostino, Chem. Mater. 18 (2006) 1561.
[8] S. Yanagida, A. Nakajima, T. Sasaki, Y. Kameshima, K. Okada, Chem. Mater. 20 (2008) 3757.
[9] X. Qu, Y. Guo, C. Hu, J. Mol. Catal. A: Chem. 262 (2007) 128.
[10] Y. Guo, C. Hu, J. Mol. Catal. A: Chem. 262 (2007) 136.
[11] T. Tachikawa, M. Fujitsuka, T. Majima, J. Phys. Chem. C 111 (2007) 5259.
[12] A. Fujishima, K. Hashimoto, T. Watanabe, TiO_2 Photocatalysis: Fundamentals and Applications, Bkc, Tokyo, 1999.
[13] M. Fernández-García, A. Martínez-Arias, J.C. Hanson, J.A. Rodríguez, Chem. Rev. 104 (2004) 4063.
[14] M. Addamo, M. Del Arco, M. Bellardita, D. Carriazo, A. Di Paola, E. García-López, G. Marcì, C. Martín, L. Palmisano, V. Rives, Res. Chem. Intermed. 33 (2007) 465.
[15] R.I. Bickley, G. Munuera, F.S. Stone, J. Catal. 31 (1973) 398.
[16] S.A. Larson, J.A. Widengree, J. Falconer, J. Catal. 157 (1995) 611.
[17] F. Arsac, D. Bianchi, J.M. Chovelon, C. Ferronato, J.M. Herrmann, J. Phys. Chem. A 110 (2006), 4202 and 4213.
[18] B. Othani, K. Iwai, S. Nishimoto, S. Sato, J. Phys. Chem. B 101 (1997) 3349.
[19] A. Sclafani, J. Herrmann, J. Photochem. Photobiol. A: Chem. 113 (1998) 181.
[20] H. Yamashita, Y. Nishida, S. Yuan, K. Mori, M. Nirisawa, Y. Matsumura, T. Ohmichi, I. Takayama, Catal. Today 120 (2007) 163.
[21] E. Ortiz-Islas, T. López, J. Navarrete, X. Bokhimi, R. Gómez, J. Mol. Catal. A: Chem. 228 (2005) 345.
[22] A. Gervasini, Y. Fenyvesi, A. Auroux, Catal. Lett. 43 (1997) 219.
[23] G. Marcì, M. Addamo, V. Augugliaro, S. Coluccia, E. García-López, V. Loddo, G. Martra, L. Palmisano, M. Schiavello, J. Photochem. Photobiol. A: Chem. 160 (2003) 105.
[24] F.P. Koffyberg, K. Dwight, A. Wold, Solid State Commun. 30 (1979) 433.
[25] Y.I. Kim, S.J. Atherton, E.S. Brigham, T.E. Mallouk, J. Phys. Chem. 97 (1993) 11802.
[26] M.T. Pope, Heteropoly and Isopolyoxometalates, Springer-Verlag, New York, 1983.
[27] C. Rocchicciolo-Deltcheff, M. Fournier, R. Franck, R. Thouvenot, Inorg. Chem. 22 (1983) 207.
[28] U. Lavrenčič Štangar, N. Grošelj, B. Orel, Ph. Colomban, Chem. Mater. 12 (2000) 3745.
[29] G. Munuera, F.S. Stone, Disc. Faraday Soc. 52 (1971) 205.
[30] G. Martra, V. Augugliaro, S. Coluccia, E. García-López, V. Loddo, L. Marchese, L. Palmisano, M. Schiavello, Stud. Surf. Sci. Catal. 130 (2000) 665.